PHYSICAL REVIEW D **96,** 056007 (2017)

Improved sensitivity on the electromagnetic dipole moments of the top quark in $\gamma\gamma$, $\gamma\gamma^*$, and $\gamma^*\gamma^*$ collisions at the CLIC

A. A. Billur,[1,*] M. Köksal,[2,†] and A. Gutiérrez-Rodríguez[3,‡]

[1]*Department of Physics, Cumhuriyet University, 58140 Sivas, Turkey*
[2]*Department of Optical Engineering, Cumhuriyet University, 58140 Sivas, Turkey*
[3]*Facultad de Física, Universidad Autónoma de Zacatecas*
Apartado Postal C-580, 98060 Zacatecas, Mexico

(Received 1 April 2017; published 12 September 2017)

We realize a phenomenological study to examine the sensitivity on the magnetic moment and electric dipole moment of the top quark through the processes $\gamma\gamma \to t\bar{t}$, $e\gamma \to e\gamma^*\gamma \to et\bar{t}$, and $e^-e^+ \to e^-\gamma^*\gamma^*e^+ \to e^-t\bar{t}e^+$ at the Compact Linear Collider (CLIC). We find that with a center-of-mass energy of the CLIC-1.4 TeV, integrated luminosity of $\mathcal{L} = 1500$ fb^{-1} and CLIC-3 TeV, integrated luminosity of $\mathcal{L} = 2000$ fb^{-1} with systematic uncertainties of $\delta_{\rm sys} = 0, 5\%, 10\%$ at the 95% C.L., it is possible the CLIC may put limits on the electromagnetic dipole moments of the top quark $\hat{a}_V$ and $\hat{a}_A$ with a sensitivity of $\mathcal{O}(10^{-3} - 10^{-2})$. Therefore, we show that the sensitivity with the CLIC data is much greater than that for the Large Hadron Collider data.

DOI: 10.1103/PhysRevD.96.056007

I. INTRODUCTION

The Standard Model (SM) has been tested in many important experiments and has been quite successful, particularly after the discovery of a particle consistent with the Higgs boson with a mass of about 125 ± 0.4 GeV. On the other hand, some of the most fundamental questions still remain unanswered. For instance, the *CP* problem, neutrino oscillations, and matter-antimatter asymmetry have not been adequately clarified by the SM. For this reason, it is often thought that the SM is embedded in a more fundamental theory with which its effects can be observed at higher energy scales.

The top quark is the most massive of all observed elementary particles in the SM. Because of the top quark's large mass, its couplings are expected to be more sensitive to new physics beyond the SM with respect to other particles. New physics can manifest itself in different forms. One possibility is that the new physics may lead to the appearance or a huge increase of new types of interactions like tH^+b or anomalous flavor changing neutral current tqg, $tq\gamma$, and tqZ ($q = u$, c) interactions. Another possibility is the modification of the SM couplings that involve $t\bar{t}g$, $t\bar{t}\gamma$, $t\bar{t}Z$, and tWb vertices.

CP violation was first discovered in a small fraction of the kaon decays. This phenomenology can easily be introduced by the Cabibbo-Kobayashi-Maskawa matrix in the quark sector. *CP* violation in this sector is not enough to clarify the baryon asymmetry in the Universe. This asymmetry is one of the basic problems in the SM that has not been resolved even in the heavy quarks decay processes. Therefore, the measurement of large amounts of *CP* violation in the top quark processes in colliders can demonstrate new physics. The existence of new physics can be analyzed by investigating the electromagnetic properties of the top quark that are determined with its dipole moments such as the magnetic dipole moment (MDM) and electric dipole moment (EDM) defined as a source of *CP* violation.

The projection in the SM for the MDM of the top quark is $a_t^{\rm SM} = 0.02$ [1], and can be tested in the current and future colliders such as the Large Hadron Collider (LHC) and the Compact Linear Collider (CLIC). In contrast, the EDM of the top quark is strongly suppressed with a value of less than 10^{-30} e cm [2–4] and is much too small to be observed. However, it is very attractive for probing new physics. If there is a new physics beyond the SM, the top quark may have a higher EDM value than 10^{-30} e cm. It is worth mentioning that the sensitivity to the EDM has been studied in models with vectorlike multiplets that predicted the top quark EDM close to 1.75×10^{-3} [5].

The studies performed through the $t\bar{t}\gamma$ production for the LHC at $\sqrt{s} = 14$ TeV, $\mathcal{L} = 300$ fb^{-1}, and 3000 fb^{-1} reported the limits of ± 0.2 and ± 0.1, respectively [6]. The limits $-2.0 \le \hat{a}_V \le 0.3$ and $-0.5 \le \hat{a}_A \le 1.5$ are obtained from the branching ratio and the *CP* asymmetry from radiative $b \to s\gamma$ transitions [7]. However, the authors of Ref. [8] obtained the bounds on $|\hat{a}_V| < 0.05(0.09)$ and $|\hat{a}_A| < 0.20(0.28)$ from measurements of the $\gamma^* p \to t\bar{t}$ cross section with 10% (18%) uncertainty at the Large Hadron electron Collider, respectively. Bounds on the dipole moments of the top quark were recently reported in literature through the process $pp \to p\gamma^*\gamma^* p \to pt\bar{t}p$ for

*abillur@cumhuriyet.edu.tr
†mkoksal@cumhuriyet.edu.tr
‡alexgu@fisica.uaz.edu.mx

 © 2017 American Physical Society

the energy and luminosity of the LHC of $\sqrt{s} = 14$ TeV, $\mathcal{L} = 3000$ fb^{-1}, and 68% C.L.: $-0.6389 \leq \hat{a}_V \leq 0.0233$ and $|\hat{a}_A| \leq 0.1158$ [9].

Moreover, in the case of the e^+e^- collider as the International Linear Collider (ILC), the sensitivity bounds at 1σ for the anomalous couplings of the top quark through top quark pair production $e^+e^- \to t\bar{t}$ at $\sqrt{s} = 500$ GeV, $\mathcal{L} = 200$ fb^{-1}, $\mathcal{L} = 300$ fb^{-1}, and $\mathcal{L} = 500$ fb^{-1} are predicted to be of the order $\mathcal{O}(10^{-3})$, indicating that measurements at an electron positron collider lead to a significant improvement in comparison with the LHC. Thorough and detailed discussions on the dipole moments of the top quark in top quark pair production at the ILC are reported in the literature [10–21]. On the other hand, the authors of Ref. [22] have found that the process $e^-e^+ \to t\bar{t}$ will do slightly better than $\gamma\gamma \to t\bar{t}$ for the determination of the anomalous $tt\gamma$ couplings.

In Ref. [23], bounds are estimated on the electromagnetic dipole moments of the top quark through the processes $\gamma e^- \to \bar{t}b\nu_e$ and $e^+e^- \to e^-\gamma^* e^+ \to \bar{t}b\nu_e e^+$ with unpolarized and polarized electron beams at the CLIC. For the systematic uncertainties of $\delta_{\rm sys} = 0\%$, 5%, $b-$tagging efficiency $= 0.8$, center-of-mass energy of $\sqrt{s} = 3$ TeV, integrated luminosity of $\mathcal{L} = 2000$ fb^{-1}, and $2\sigma(3\sigma)$, the bounds obtained on the electromagnetic dipole moments $\hat{a}_V$ and $\hat{a}_A$ of the top quark are of the order $\mathcal{O}(10^{-2} - 10^{-1})$ and are highly competitive with those reported in previous studies.

The advantage of the linear e^-e^+ colliders with respect to the hadron colliders is in the general cleanliness of the events where two elementary particles, electron and positron beams, collide at high energy, and the high resolutions of the detector are made possible by the relatively low absolute rate of background events. In addition, these colliders will complement the physics program of the LHC, especially for precision physics. Therefore, precise measurements of the top quark properties, such as the mass, charge, spin, and dipole moments will become possible. The CLIC is a proposed future e^-e^+ collider, designed to fulfill e^-e^+ collisions at center-of-mass energies of 0.35, 1.4, and 3 TeV planned to be constructed with a three main stage research region [24]. This enables the investigation of the $\gamma\gamma$ and $e\gamma$ interactions by converting the original e^- or e^+ beam into a photon beam through the Compton backscattering mechanism. The other well-known applications of the linear colliders are the processes $e\gamma^*$, $\gamma\gamma^*$, $\gamma^*\gamma^*$ where the emitted quasireal photon γ^* is scattered with small angles from the beam pipe of e^- or e^+ [25–30]. Since these photons have a low virtuality, they are almost on the mass shell. These processes can be described by the Weizsacker-Williams approximation (WWA). The WWA has a lot of advantages such as providing the skill to reach crude numerical predictions via simple formulas. In addition, it may principally ease the experimental analysis because it enables one to directly achieve a rough cross section for the $\gamma^*\gamma^* \to X$ process via the examination of the main process $e^-e^+ \to e^-Xe^+$ where X represents objects produced in the final state. The production of high mass objects is particularly interesting at the linear colliders, and the production rate of massive objects is limited by the photon luminosity at high invariant mass while $\gamma^*\gamma^*$ and $e\gamma^*$ processes at the linear colliders arise from the quasireal photon emitted from the incoming beams. Hence, $\gamma^*\gamma^*$ and $e\gamma^*$ are more realistic than $\gamma\gamma$ and $e\gamma$. These processes have been observed experimentally at LEP, Tevatron, and LHC [31–65].

In this paper, we perform a phenomenological study for determining the sensitivity on the magnetic moment and electric dipole moment of the top quark through the $t\bar{t}$ pair production in e^+e^- colliders, specifically for center-of-mass energy and luminosity of CLIC-1.4 TeV, $\mathcal{L} = 1500$ bf^{-1} and CLIC-3 TeV, $\mathcal{L} = 2000$ bf^{-1} with systematic uncertainty of $\delta_{\rm sys} = 0$, 5%, 10%, and 95% C.L. Here, we consider that the top quark pair production in e^+e^- interactions is given through three different processes $\gamma\gamma \to t\bar{t}$, $e\gamma \to e\gamma^*\gamma \to et\bar{t}$, $e^-e^+ \to e^-\gamma^*\gamma^* e^+ \to e^-t\bar{t}e^+$ where γ and γ^* are Compton backscattered and Weizsacker-Williams photons, respectively. These processes are one of the most important sources of $t\bar{t}$ pair production and may represent new physics effects at a high energy and high luminosity linear electron positron collider such as the CLIC and also isolate anomalous $t\bar{t}\gamma$ coupling from $t\bar{t}Z$.

This work is structured as follows. In Sec. II, we introduce the top quark effective electromagnetic interactions. In Sec. III, we study the dipole moments of the top quark through the processes $\gamma\gamma \to t\bar{t}$, $e\gamma \to e\gamma^*\gamma \to et\bar{t}$, and $e^-e^+ \to e^-\gamma^*\gamma^* e^+ \to e^-t\bar{t}e^+$. Finally, we present our conclusions in Sec. IV.

II. TOP QUARK PAIR PRODUCTION PROCESSES IN PHOTON-PHOTON COLLISIONS

A. General effective coupling $t\bar{t}\gamma$

The most general effective coupling $t\bar{t}\gamma$ which includes the SM coupling and contributions from dimension-six effective operators can be written as [6,9,66–68]

$$\mathcal{L}_{t\bar{t}\gamma} = -g_e Q_t \bar{t}\Gamma^\mu_{t\bar{t}\gamma} t A_\mu, \tag{1}$$

where g_e is the electromagnetic coupling constant, Q_t is the top quark electric charge, and the Lorentz-invariant vertex function $\Gamma^\mu_{t\bar{t}\gamma}$, which describes the interaction of a γ photon with two top quarks, can be parametrized by

$$\Gamma^\mu_{t\bar{t}\gamma} = \gamma^\mu + \frac{i}{2m_t}(\hat{a}_V + i\hat{a}_A\gamma_5)\sigma^{\mu\nu}q_\nu, \tag{2}$$

where m_t is the mass of the top quark, q is the momentum transfer to the photon, and the couplings $\hat{a}_V$ and $\hat{a}_A$ are real and related to the anomalous magnetic moment and the electric dipole moment of the top quark, respectively.

B. Theoretical calculations

Schematic diagrams for the processes $e\gamma \to e\gamma^*\gamma \to et\bar{t}$ and $e^-e^+ \to e^-\gamma^*\gamma^*e^+ \to e^-t\bar{t}e^+$ are given in Fig. 1. With these processes, $\gamma(\gamma^*)\gamma(\gamma^*) \to t\bar{t}$ have two Feynman diagrams that are shown in detail in Fig. 2.

For $\gamma\gamma$, $\gamma\gamma^*$, and $\gamma^*\gamma^*$ collisions including the effective Lagrangian in Eq. (1), the polarization summed amplitude square is given in a function of the Mandelstam invariants $\hat{s}$, $\hat{t}$, and $\hat{u}$ as follows:

$$|M_1|^2 = \frac{16\pi^2 Q_t^2 \alpha_e^2}{2m_t^4(\hat{t}-m_t^2)^2}[48\hat{a}_V(m_t^2-\hat{t})(m_t^2+\hat{s}-\hat{t})m_t^4 - 16(3m_t^4 - m_t^2\hat{s} + \hat{t}(\hat{s}+\hat{t}))m_t^4 + 2(m_t^2-\hat{t})(\hat{a}_V^2(17m_t^4+(22\hat{s}-26\hat{t})m_t^2+\hat{t}(9\hat{t}-4\hat{s})) + \hat{a}_A^2(17m_t^2+4\hat{s}-9\hat{t})(m_t^2-\hat{t}))m_t^2 + 12\hat{a}_V(\hat{a}_V^2+\hat{a}_A^2)\hat{s}(m_t^3-m_t\hat{t})^2 - (\hat{a}_V^2+\hat{a}_A^2)^2(m_t^2-\hat{t})^3(m_t^2-\hat{s}-\hat{t})], \quad (3)$$

$$|M_2|^2 = \frac{-16\pi^2 Q_t^2 \alpha_e^2}{2m_t^4(\hat{u}-m_t^2)^2}[48\hat{a}_V(m_t^4+(\hat{s}-2\hat{t})m_t^2+\hat{t}(\hat{s}+\hat{t}))m_t^4 + 16(7m_t^4-(3\hat{s}+4\hat{t})m_t^2+\hat{t}(\hat{s}+\hat{t}))m_t^4 + 2(m_t^2-\hat{t})(\hat{a}_V^2(m_t^4+(17\hat{s}-10\hat{t})m_t^2+9\hat{t}(\hat{s}+\hat{t})) + \hat{a}_A^2(m_t^2-9\hat{t})(m_t^2-\hat{t}-\hat{s}))m_t^2 + (\hat{a}_V^2+\hat{a}_A^2)^2(m_t^2-\hat{t})^3(m_t^2-\hat{s}-\hat{t})], \quad (4)$$

$$M_1^\dagger M_2 + M_2^\dagger M_1 = \frac{16\pi^2 Q_t^2 \alpha_e^2}{m_t^2(\hat{t}-m_t^2)(\hat{u}-m_t^2)}[-16(4m_t^6 - m_t^4\hat{s}) + 8\hat{a}_V m_t^2(6m_t^4 - 6m_t^2(\hat{s}+2\hat{t})-\hat{s})^2 + 6\hat{t})^2 + 6\hat{s}\,\hat{t}) + (\hat{a}_V^2(16m_t^6 - m_t^4(15\hat{s}+32\hat{t}) + m_t^2(15\hat{s})^2 + 14\hat{t}\,\hat{s} + 16\hat{t})^2) + \hat{s}\,\hat{t}(\hat{s}+\hat{t})) + \hat{a}_A^2(16m_t^6 - m_t^4(15\hat{s}+32\hat{t}) + m_t^2(5\hat{s})^2 + 14\hat{t}\,\hat{s} + 16\hat{t})^2) + \hat{s}\,\hat{t}(\hat{s}+\hat{t}))) - 4\hat{a}_V\hat{s}(\hat{a}_V^2+\hat{a}_A^2)(m_t^4+m_t^2(\hat{s}-2\hat{t})+\hat{t}(\hat{s}+\hat{t})) - 4\hat{a}_A(\hat{a}_V^2+\hat{a}_A^2)(2m_t^2-\hat{s}-2\hat{t})\epsilon_{\alpha\beta\gamma\delta}p_1^\alpha p_2^\beta p_3^\gamma p_4^\delta - 2\hat{s}(\hat{a}_V^2+\hat{a}_A^2)^2(m_t^4-2\hat{t}m_t^2+\hat{t}(\hat{s}+\hat{t}))], \quad (5)$$

where $\hat{s} = (p_1+p_2)^2 = (p_3+p_4)^2$, $\hat{t} = (p_1-p_3)^2 = (p_4-p_2)^2$, $\hat{u} = (p_3-p_2)^2 = (p_1-p_4)^2$, and p_1 and p_2 are the four-momenta of the incoming photons, p_3 and p_4 are the momenta of the outgoing top quarks, Q_t is the top quark charge, $\alpha_e = g_e^2/4\pi$ is the fine-structure constant, m_t is the mass of the top, and $\hat{a}_V$ ($\hat{a}_A$) are their dipole moments.

The most promising mechanism to generate energetic photon beams in a linear collider is Compton backscattering. Compton backscattered photons interact with each other and generate the process $\gamma\gamma \to t\bar{t}$. The spectrum of Compton backscattered photons is given by

$$f_\gamma(y) = \frac{1}{g(\zeta)}\left[1-y+\frac{1}{1-y}-\frac{4y}{\zeta(1-y)}+\frac{4y^2}{\zeta^2(1-y)^2}\right], \quad (6)$$

where

$$g(\zeta) = \left(1-\frac{4}{\zeta}-\frac{8}{\zeta^2}\right)\log(\zeta+1)+\frac{1}{2}+\frac{8}{\zeta}-\frac{1}{2(\zeta+1)^2}, \quad (7)$$

with

$$y = \frac{E_\gamma}{E_e}, \quad \zeta = \frac{4E_0E_e}{M_e^2}, \quad y_{\max} = \frac{\zeta}{1+\zeta}. \quad (8)$$

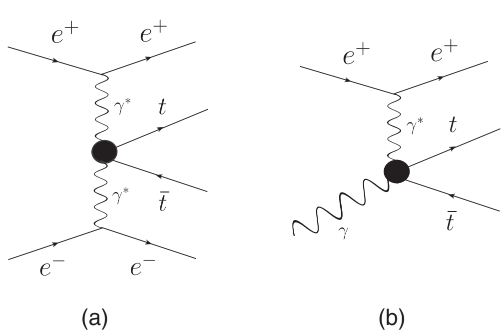

FIG. 1. A schematic diagram for the processes (a) $e^-e^+ \to e^-\gamma^*\gamma^*e^+ \to e^-t\bar{t}e^+$ and (b) $e^+\gamma \to e^+\gamma^*\gamma \to e^+t\bar{t}$.

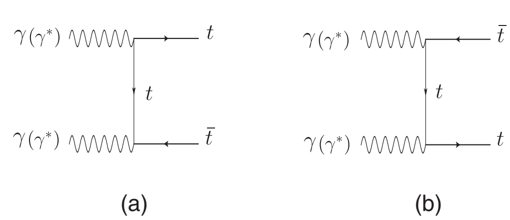

FIG. 2. Feynman diagrams contributing to the process $\gamma\gamma \to t\bar{t}$ and the subprocesses $\gamma\gamma^* \to t\bar{t}$ and $\gamma^*\gamma^* \to t\bar{t}$.

Here, E_0 and E_e are energies of the incoming laser photon and initial energy of the electron beam before Compton backscattering, and E_γ is the energy of the backscattered photon. The maximum value of y reaches 0.83 when $\zeta = 4.8$.

WWA is another possibility for top pair production. The quasireal photons emitted from both lepton beams collide with each other and produce the process $\gamma^*\gamma^* \to t\bar{t}$. In WWA, the photon spectrum is given by

$$f_{\gamma^*}(x) = \frac{\alpha}{\pi E_e}\left\{\left[\frac{1-x+x^2/2}{x}\right]\log\left(\frac{Q^2_{\rm max}}{Q^2_{\rm min}}\right) - \frac{m_e^2 x}{Q^2_{\rm min}}\left(1-\frac{Q^2_{\rm min}}{Q^2_{\rm max}}\right) - \frac{1}{x}\left[1-\frac{x}{2}\right]^2\log\left(\frac{x^2E_e^2+Q^2_{\rm max}}{x^2E_e^2+Q^2_{\rm min}}\right)\right\}, \quad (9)$$

where $x = E_\gamma/E_e$ and $Q^2_{\rm max}$ is the maximum virtuality of the photon. In this work, we have taken into account the maximum virtuality of the photon is $Q^2_{\rm max} = 2\ {\rm GeV}^2$. The larger values of $Q^2_{\rm max}$ do not make a significant contribution to the sensitivity limits, which is similar to results in previous works [69–72]. The minimum value of the $Q^2_{\rm min}$ is given by

$$Q^2_{\rm min} = \frac{m_e^2 x^2}{1-x}. \quad (10)$$

The $Q^2_{\rm min}$ value is very small due to the electron mass. However, the scattering angles of the electrons are so small that the transverse momentum is close to zero. Because of the momentum conservation, the transverse momentum of the emitted photons also have small values. In light of all these arguments, virtuality of the photons in WWA is very small, and the photons are almost on mass shell.

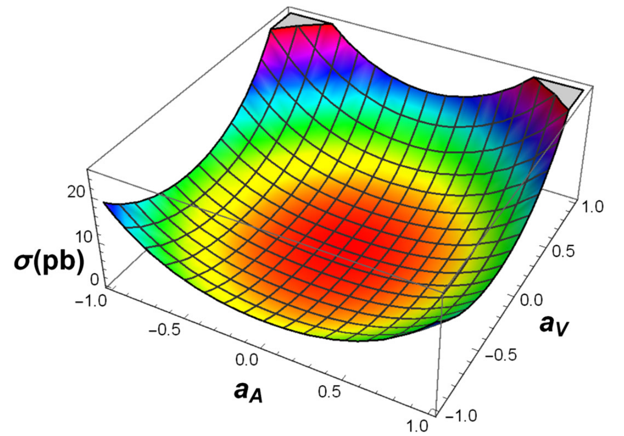

FIG. 4. Same as in Fig. 3, but for center-of-mass energy of $\sqrt{s} = 3$ TeV.

The process $\gamma^*\gamma^* \to t\bar{t}$ participates as a subprocess in the main process $e^-e^+ \to e^-\gamma^*\gamma^*e^+ \to e^-t\bar{t}e^+$. However, an γ^* photon emitted from either of the incoming leptons can interact with the Compton backscattered photon, and the subprocess $\gamma\gamma^* \to t\bar{t}$ can take place. Hence, we calculate the process $e\gamma \to e\gamma^*\gamma \to et\bar{t}$ by integrating the cross section for the subprocess $\gamma\gamma^* \to t\bar{t}$.

The total cross sections are

$$\sigma = \int f_{\gamma(\gamma^*)}(x) f_{\gamma(\gamma^*)}(x) d\hat{\sigma} dE_1 dE_2. \quad (11)$$

The total cross sections of these processes as functions of anomalous $\hat{a}_V$ and $\hat{a}_A$ are shown in Figs. 3–8. We understand from Figs. 3–8 that the total cross sections show a clear dependence on the dipole moments of the top quark. Anomalous $\hat{a}_V$ and $\hat{a}_A$ parameters have different CP properties that can be seen in Eqs. (3)–(5). The cross section with respect to the $\hat{a}_A$ parameter is even power and a nonzero value of this parameter allows a constructive effect

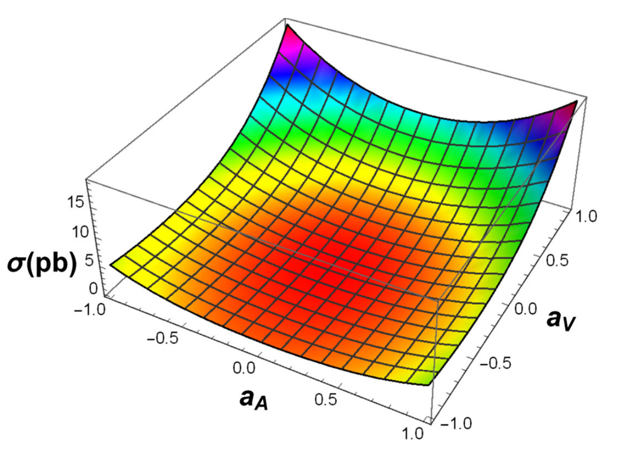

FIG. 3. The total cross sections of the process $\gamma\gamma \to t\bar{t}$ as a function of $\hat{a}_V$ and $\hat{a}_A$ for center-of-mass energy of $\sqrt{s} = 1.4$ TeV.

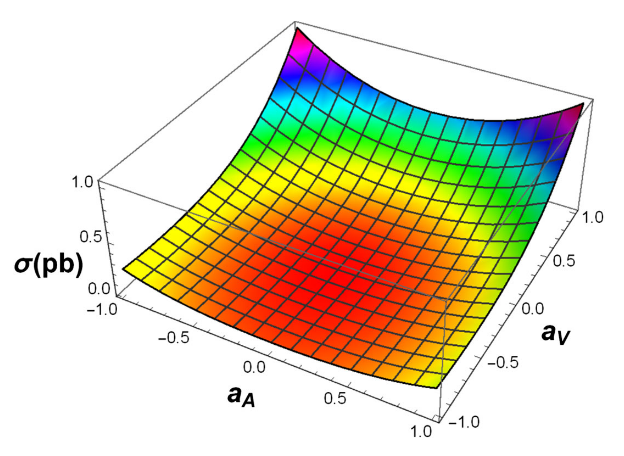

FIG. 5. The total cross sections of the process $e^+\gamma \to e^+\gamma^*\gamma \to e^+t\bar{t}$ as a function of $\hat{a}_V$ and $\hat{a}_A$ for center-of-mass energy of $\sqrt{s} = 1.4$ TeV.

TABLE I. Numerical computations of the total cross sections versus $\hat{a}_V$ and $\hat{a}_A$ at $\sqrt{s} = 3$ TeV.

Mode	σ_4	σ_3	σ_2	σ_1	σ_0	σ'_4	σ'_2
$\gamma\gamma \to t\bar{t}$	4.52	4.51	5.24	0.97	0.38	4.52	4.75
$e^+\gamma \to e^+\gamma^*\gamma \to e^+t\bar{t}$	0.24	0.42	0.56	0.19	0.07	0.24	0.46
$e^+e^- \to e^+\gamma^*\gamma^*e^- \to e^+t\bar{t}e^-$	0.012	0.027	0.039	0.016	0.006	0.012	0.031

on the total cross section. In addition, the contribution of $\hat{a}_V$ coupling to the cross sections is proportional to odd power. In Fig. 3, there are small intervals around $\hat{a}_V$ in which the cross section that includes new physics is smaller than the SM cross section. For this reason, the $\hat{a}_V$ parameter has a partially destructive effect on the total cross section.

The scattering amplitudes can be given in Eqs. (3)–(5) as a polynomial in powers of $\hat{a}_V(\hat{a}_A)$. Therefore, the cross section as a polynomial in powers of $\hat{a}_V(\hat{a}_A)$ for the three modes $\gamma\gamma \to t\bar{t}$, $e^+\gamma \to e^+\gamma^*\gamma \to e^+t\bar{t}$, and $e^+e^- \to e^+\gamma^*\gamma^*e^- \to e^+t\bar{t}e^-$ are given by

$$\sigma_{Tot}(\hat{a}_V) = \sigma_4\hat{a}_V^4 + \sigma_3\hat{a}_V^3 + \sigma_2\hat{a}_V^2 + \sigma_1\hat{a}_V^1 + \sigma_0, \quad (12)$$

$$\sigma_{Tot}(\hat{a}_A) = \sigma'_4\hat{a}_A^4 + \sigma'_2\hat{a}_A^2 + \sigma_0, \quad (13)$$

where $\sigma^i(\sigma'_i)$ $i = 1, \ldots, 4$ is the anomalous contribution, while σ_0 is the contribution of the SM at $\hat{a}_V = \hat{a}_A = 0$, respectively. This provides more precise and convenient information for each process. The numerical computations of the coefficients of $\hat{a}_V$ and $\hat{a}_A$ of Eqs. (12) and (13) are presented in Table I.

When comparing the three processes in Figs. 3–8, the largest deviation from the SM of the anomalous cross sections, including anomalous $\hat{a}_V$ and $\hat{a}_A$ couplings, is the process $\gamma\gamma \to t\bar{t}$. The best sensitivities on anomalous $\hat{a}_V$ and $\hat{a}_A$ couplings are obtained from the process $\gamma\gamma \to t\bar{t}$. Similarly, the sensitivities obtained on anomalous couplings through the process $e\gamma \to e\gamma^*\gamma \to et\bar{t}$ are expected to be more restrictive than the sensitivities on the process $e^-e^+ \to e^-\gamma^*\gamma^*e^+ \to e^-t\bar{t}e^+$.

When making a direct comparison of our results for the total cross section as a function of the dipole moments $\hat{a}_V$ and $\hat{a}_A$ reported in Figs. 3–8 with those reported in Ref. [9] (see Figs. 3 and 4), we find that our results, using processes $\gamma\gamma \to t\bar{t}$, $\gamma\gamma^* \to t\bar{t}$, and $\gamma^*\gamma^* \to t\bar{t}$ at CLIC energies, with respect to process $pp \to p\gamma^*\gamma^*p \to pt\bar{t}p$ at LHC energies, show a significant improvement. In addition, with our processes the total cross sections are of 3–4 orders of magnitude better than those reported in Ref. [9]. This shows that the bounds on the anomalous couplings $\hat{a}_V$ and $\hat{a}_A$ can be improved at a linear collider such as the CLIC by a few orders of magnitude when compared to what is possible at the LHC.

III. DIPOLE MOMENTS OF THE TOP QUARK IN $\gamma\gamma$, $\gamma\gamma^*$, AND $\gamma^*\gamma^*$ COLLISIONS

To investigate the sensitivity to the anomalous $\hat{a}_V$ and $\hat{a}_A$ couplings we use the chi-squared distribution,

$$\chi^2 = \left(\frac{\sigma_{\rm SM} - \sigma_{\rm NP}(\hat{a}_V, \hat{a}_A)}{\sigma_{\rm SM}\delta}\right)^2, \quad (14)$$

where $\sigma_{\rm NP}(\hat{a}_V, \hat{a}_A)$ is the total cross section including contributions from the SM and new physics, $\delta = \sqrt{(\delta_{st})^2 + (\delta_{\rm sys})^2}$, $\delta_{st} = \frac{1}{\sqrt{N_{\rm SM}}}$ is the statistical error, and $\delta_{\rm sys}$ is the systematic error. The number of events for each of the three processes is given by $N_{\rm SM} = \mathcal{L}_{\rm int} \times BR \times \sigma_{\rm SM} \times \epsilon_{b\text{-tag}} \times \epsilon_{b\text{-tag}}$, where $\mathcal{L}_{\rm int}$ is the integrated luminosity and b-jet tagging efficiency is 0.8 [73]. The top quarks decay almost 100% to W boson and b quark. For top quark pair production we can categorize decay products according to the decomposition of W. In this work, we assume that one of the W bosons decays leptonically and the other hadronically for the signal. This phenomenon has already been studied by ATLAS and CMS Collaborations [74–76]. Thus, we assume that the branching ratio of the top quark pair in the final state is BR = 0.286.

For our numerical computation, we take a set of independent input parameters that are known from current experiments. The input parameters are $\alpha = \frac{1}{137.4}$, $m_b = 4.18$ GeV, and $m_t = 173.21$ GeV [77], and for our analysis, we consider a 95% C.L. sensitivity on the dipole moments $\hat{a}_V$ and $\hat{a}_A$ of the top quark via the processes $\gamma\gamma \to t\bar{t}$, $e\gamma \to e\gamma^*\gamma \to et\bar{t}$, and $e^-e^+ \to e^-\gamma^*\gamma^*e^+ \to e^-t\bar{t}e^+$ at the CLIC-1.4 TeV with $\mathcal{L}_{\rm int} = 1500$ fb^{-1} and CLIC-3 TeV with $\mathcal{L}_{\rm int} = 2000$ fb^{-1}.

Tables II–VII illustrate the sensitivity obtained at 95% C.L. on the dipole moments $\hat{a}_V$ and $\hat{a}_A$ of the top quark through the processes $\gamma\gamma \to t\bar{t}$, $e\gamma \to e\gamma^*\gamma \to et\bar{t}$, and $e^-e^+ \to e^-\gamma^*\gamma^*e^+ \to e^-t\bar{t}e^+$. The bounds are obtained assuming that the center-of-mass energy of CLIC-1.4 TeV and luminosities of $\mathcal{L} = 50$, 300, 500, 1000, 1500 fb^{-1} for the second stage of operation of the collider. For the third stage, we consider the center-of-mass energy of CLIC-3 TeV and luminosities of $\mathcal{L} = 50$, 300, 500, 1000, 1500, 2000 fb^{-1}.

An important part of our analysis is the inclusion of theoretical uncertainties as there may be several experimental and systematic uncertainty sources in top quark

TABLE II. Sensitivity on the $\hat{a}_V$ magnetic moment and the $\hat{a}_A$ electric dipole moment for the process $\gamma\gamma \to t\bar{t}$.

$\sqrt{s} = 1.4$ TeV, 95% C.L.			
$\mathcal{L}(\mathrm{fb}^{-1})$	δ_{sys}	$\hat{a}_V$	$\lvert\hat{a}_A\rvert$
500	0%	[−0.5170, 0.0034]	0.0385
500	5%	[−0.5650, 0.0347]	0.1286
500	10%	[−0.6122, 0.0641]	0.1811
1000	0%	[−0.5155, 0.0024]	0.0324
1000	5%	[−0.5649, 0.0346]	0.1285
1000	10%	[−0.6122, 0.0641]	0.1811
1500	0%	[−0.5149, 0.0020]	0.0293
1500	5%	[−0.5648, 0.0346]	0.1284
1500	10%	[−0.6121, 0.0640]	0.1811

identification. This situation has not been studied experimentally in linear colliders. For hadron colliders, especially LHC, the process of determining the cross section of top pair production has been experimentally studied [78,79]. As seen from these studies, the total systematic uncertainty value is about 10% and is increasingly

TABLE III. Sensitivity on the $\hat{a}_V$ magnetic moment and the $\hat{a}_A$ electric dipole moment for the process $\gamma\gamma \to t\bar{t}$.

$\sqrt{s} = 3$ TeV, 95% C.L.			
$\mathcal{L}(\mathrm{fb}^{-1})$	δ_{sys}	$\hat{a}_V$	$\lvert\hat{a}_A\rvert$
500	0%	[−0.2225, 0.0040]	0.0291
500	5%	[−0.2564, 0.0331]	0.0892
500	10%	[−0.2870, 0.0585]	0.1254
1000	0%	[−0.2212, 0.0029]	0.0245
1000	5%	[−0.2563, 0.0330]	0.0891
1000	10%	[−0.2869, 0.0585]	0.1254
1500	0%	[−0.2206, 0.0024]	0.0221
1500	5%	[−0.2563, 0.0330]	0.0890
1500	10%	[−0.2869, 0.0585]	0.1254
2000	0%	[−0.2203, 0.0020]	0.0206
2000	5%	[−0.2563, 0.0330]	0.0879
2000	10%	[−0.2869, 0.0585]	0.1254

TABLE IV. Sensitivity on the $\hat{a}_V$ magnetic moment and the $\hat{a}_A$ electric dipole moment for the process $e\gamma \to e\gamma^*\gamma \to et\bar{t}$.

$\sqrt{s} = 1.4$ TeV, 95% C.L.			
$\mathcal{L}(\mathrm{fb}^{-1})$	δ_{sys}	$\hat{a}_V$	$\lvert\hat{a}_A\rvert$
500	0%	[−0.7300, 0.0121]	0.0848
500	5%	[−0.7717, 0.0358]	0.1496
500	10%	[−0.8244, 0.0647]	0.2068
1000	0%	[−0.7241, 0.0086]	0.0713
1000	5%	[−0.7701, 0.0349]	0.1477
1000	10%	[−0.8236, 0.0643]	0.2061
1500	0%	[−0.7215, 0.0070]	0.0644
1500	5%	[−0.7697, 0.0346]	0.1470
1500	10%	[−0.8234, 0.0641]	0.2059

TABLE V. Sensitivity on the $\hat{a}_V$ magnetic moment and the $\hat{a}_A$ electric dipole moment for the process $e\gamma \to e\gamma^*\gamma \to et\bar{t}$.

$\sqrt{s} = 3$ TeV, 95% C.L.			
$\mathcal{L}(\mathrm{fb}^{-1})$	δ_{sys}	$\hat{a}_V$	$\lvert\hat{a}_A\rvert$
500	0%	[−0.4626, 0.0088]	0.0610
500	5%	[−0.4961, 0.0034]	0.1249
500	10%	[−0.5333, 0.0630]	0.1740
1000	0%	[−0.4593, 0.0063]	0.0512
1000	5%	[−0.4955, 0.0343]	0.1240
1000	10%	[−0.5332, 0.0629]	0.1737
1500	0%	[−0.4579, 0.0052]	0.0463
1500	5%	[−0.4953, 0.0342]	0.1237
1500	10%	[−0.5331, 0.0628]	0.1736
2000	0%	[−0.4570, 0.0045]	0.0431
2000	5%	[−0.4952, 0.0341]	0.1236
2000	10%	[−0.5330, 0.0627]	0.1735

TABLE VI. Sensitivity on the $\hat{a}_V$ magnetic moment and the $\hat{a}_A$ electric dipole moment for the process $e^-e^+ \to e^-\gamma^*\gamma^*e^+ \to e^-t\bar{t}e^+$.

$\sqrt{s} = 1.4$ TeV, 95% C.L.			
$\mathcal{L}(\mathrm{fb}^{-1})$	δ_{sys}	$\hat{a}_V$	$\lvert\hat{a}_A\rvert$
500	0%	[−0.9123, 0.0490]	0.1878
500	5%	[−0.9298, 0.0580]	0.2057
500	10%	[−0.9690, 0.0774]	0.2415
1000	0%	[−0.8859, 0.0357]	0.1581
1000	5%	[−0.9090, 0.0478]	0.1850
1000	10%	[−0.9558, 0.0709]	0.2299
1500	0%	[−0.8739, 0.0295]	0.1429
1500	5%	[−0.9014, 0.0437]	0.1762
1500	10%	[−0.9510, 0.0686]	0.2256

TABLE VII. Sensitivity on the $\hat{a}_V$ magnetic moment and the $\hat{a}_A$ electric dipole moment for the process $e^-e^+ \to e^-\gamma^*\gamma^*e^+ \to e^-t\bar{t}e^+$.

$\sqrt{s} = 3$ TeV, 95% C.L.			
$\mathcal{L}(\mathrm{fb}^{-1})$	δ_{sys}	$\hat{a}_V$	$\lvert\hat{a}_A\rvert$
500	0%	[−0.6212, 0.0291]	0.1259
500	5%	[−0.6417, 0.0434]	0.1561
500	10%	[−0.6773, 0.0679]	0.2000
1000	0%	[−0.6097, 0.0210]	0.1059
1000	5%	[−0.6353, 0.0390]	0.1472
1000	10%	[−0.6739, 0.0656]	0.1962
1500	0%	[−0.6044, 0.0173]	0.0957
1500	5%	[−0.6330, 0.0374]	0.1439
1500	10%	[−0.6728, 0.0648]	0.1948
2000	0%	[−0.6013, 0.0151]	0.0890
2000	5%	[−0.6317, 0.0365]	0.1420
2000	10%	[−0.6721, 0.0644]	0.1942

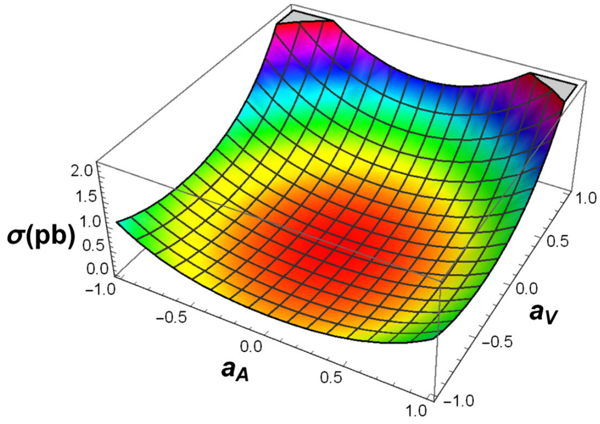

FIG. 6. Same as in Fig. 5, but for center-of-mass energy of $\sqrt{s} = 3$.

improved when it is compared with previous experimental studies [76].

We use three scenarios for the systematic uncertainties in our entire set of tables: (1) we assume a systematic uncertainty of $\delta_{\rm sys} = 0\%$, (2) we estimate future results for $\hat{a}_V$ and $\hat{a}_A$ with 5% systematic uncertainty, and (3) we consider a systematic uncertainty of as much as $\delta_{\rm sys} = 10\%$. We find in Tables II–VII that the most prominent mode of top quark pair production that imposes stronger limits on the dipole moments is the production process $\gamma\gamma \to t\bar{t}$, followed in order of importance by the processes $e\gamma \to e\gamma^*\gamma \to et\bar{t}$ and $e^-e^+ \to e^-\gamma^*\gamma^*e^+ \to e^-t\bar{t}e^+$, respectively. In conclusion, it is possible that the CLIC may put limits on the electromagnetic dipole moments of the top quark with a sensitivity of the order $\mathcal{O}(10^{-3} - 10^{-2})$ at the 95% C.L. We can see from Figs. 3–8, the cross section for the negative values of the $\hat{a}_v$ are smaller than their positive values. This can easily be seen on sensitivity tables: the bounds for the negative values of the $\hat{a}_v$ for increasing luminosity values do not change much.

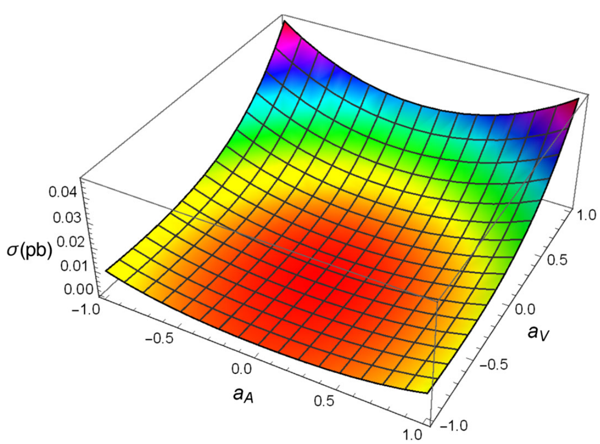

FIG. 7. The total cross sections of the process $e^+e^- \to e^+\gamma^*\gamma^*e^- \to e^+t\bar{t}e^-$ as a function of $\hat{a}_V$ and $\hat{a}_A$ for center-of-mass energy of $\sqrt{s} = 1.4$ TeV.

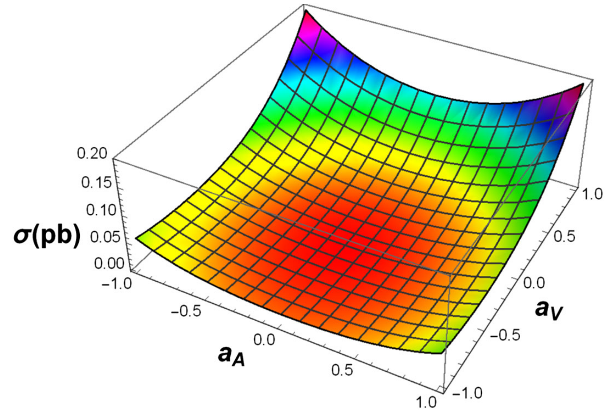

FIG. 8. Same as in Fig. 7, but for center-of-mass energy of $\sqrt{s} = 3$.

It is worthwhile to compare the results obtained here with those of Ref. [9], which consider the process $pp \to p\gamma^*\gamma^*p \to pt\bar{t}p$ with the LHC running at $\sqrt{s} = 14, 33$ TeV and with integrated luminosities of $\mathcal{L} = 100$, 300, 3000 fb^{-1}. Varying one coupling at a time, they find constraints at 68% C.L. of the order $\mathcal{O}(10^{-2} - 10^{-1})$. We also note that, while we do consider three systematic errors in our study, the quoted sensitivities in Ref. [9] do not include theoretical uncertainty. Also, the CLIC sensitivity is even better for our processes than for those reported in Ref. [9].

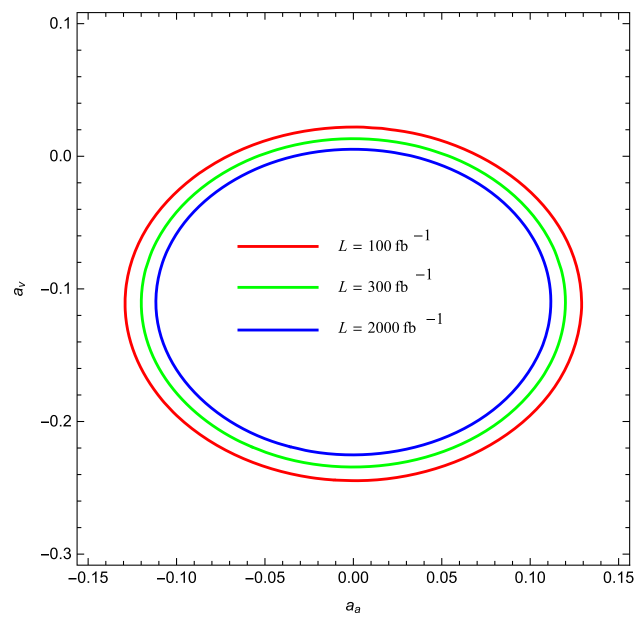

FIG. 9. Bounds contours at the 68% C.L. in the $\hat{a}_V - \hat{a}_A$ plane for the process $\gamma\gamma \to t\bar{t}$ with the $\delta_{\rm sys} = 0\%$ and for center-of-mass energy of $\sqrt{s} = 3$.

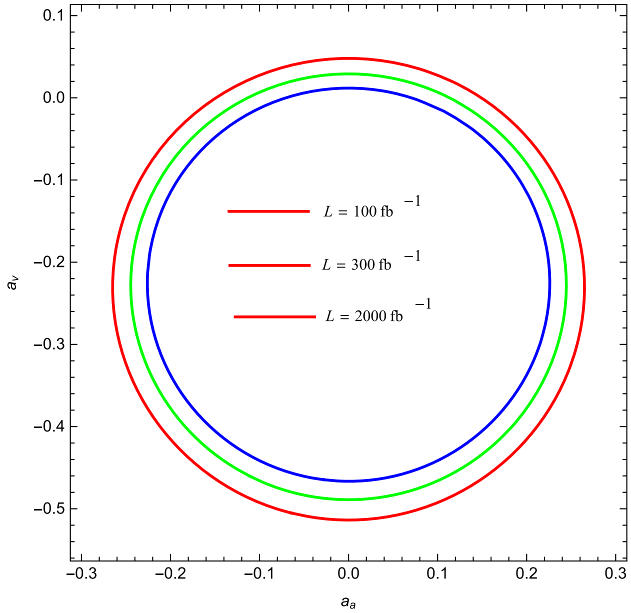

FIG. 10. Bounds contours at the 68% C.L. in the $\hat{a}_V - \hat{a}_A$ plane for $e^+e^- \to e^+\gamma\gamma^* e^- \to e^+ t\bar{t} e^-$ with the $\delta_{\rm sys} = 0\%$ and for center-of-mass energy of $\sqrt{s} = 3$.

Finally, in Figs. 9–11 we show the 95% C.L. contours for anomalous $\hat{a}_V - \hat{a}_A$ couplings for the processes $\gamma\gamma \to t\bar{t}$, $e\gamma \to e\gamma^*\gamma \to et\bar{t}$, and $e^-e^+ \to e^-\gamma^*\gamma^* e^+ \to e^- t\bar{t} e^+$ at the CLIC for various integrated luminosities and center-of-mass energies. Among the three combinations shown in these figures, we find that the strongest simultaneous limits come from the reaction $\gamma\gamma \to t\bar{t}$ at the CLIC-3 TeV and $\mathcal{L}_{\rm int} = 2000$ fb^{-1} with the 3σ level.

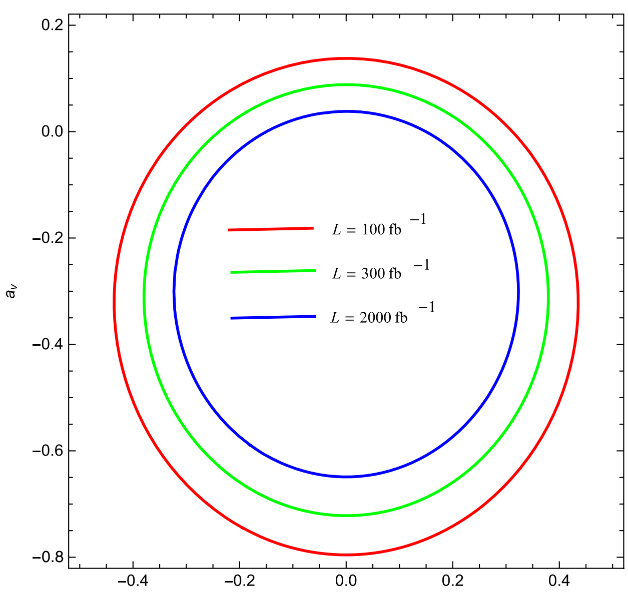

FIG. 11. Bounds contours at the 68% C.L. in the $\hat{a}_V - \hat{a}_A$ plane for $e^+e^- \to e^+\gamma^*\gamma^* e^- \to e^+ t\bar{t} e^-$ with the $\delta_{\rm sys} = 0\%$ and for center-of-mass energy of $\sqrt{s} = 3$.

IV. CONCLUSIONS

The LHC is expected to provide answers to some fundamental questions of the SM. However, high precision measurements may not be available due to remnants from the strong interactions of proton-proton collisions. For this reason, the linear collider with high luminosity and energy is a good choice to complement and extend the LHC physics program. This collider with high luminosity and energy is extremely important to examine new physics beyond the SM. The anomalous $t\bar{t}\gamma$ couplings have very strong energy dependencies since they are characterized by effective Lagrangians that contrain dimensional-high operators. Thus, the cross section including the anomalous $t\bar{t}\gamma$ coupling has a higher energy dependence than the SM cross section. The anomalous $t\bar{t}\gamma$ coupling can be analyzed through the process $e^-e^+ \to t\bar{t}$ at the linear colliders. This process receives contributions from both anomalous $t\bar{t}\gamma$ and $t\bar{t}Z$ couplings. However, the processes $\gamma\gamma \to t\bar{t}$, $e\gamma \to e\gamma^*\gamma \to et\bar{t}$, and $e^-e^+ \to e^-\gamma^*\gamma^* e^+ \to e^- t\bar{t} e^+$ isolate $t\bar{t}\gamma$ coupling that provides the possibility to analyze the $t\bar{t}\gamma$ coupling separately from the $t\bar{t}Z$ coupling. Any signal that conflicts with the SM predictions would be convincing evidence for new physics effects in $t\bar{t}\gamma$.

In this paper, we carry out a phenomenological study to investigate the sensitivity of the CLIC to the anomalous $t\bar{t}\gamma$ coupling through the $\gamma\gamma$, $\gamma\gamma^*$, and $\gamma^*\gamma^*$ collision modes followed by the semileptonic decay of the top pair production. We find that with a center-of-mass energy of CLIC-1.4 TeV, integrated luminosity of $\mathcal{L} = 1500$ fb^{-1} and CLIC-3 TeV, and integrated luminosity of $\mathcal{L} = 2000$ fb^{-1} with systematic uncertainties of $\delta_{\rm sys} = 0$, 5%, 10% at the 95% C. L., it is possible that the CLIC may put limits on the electromagnetic dipole moments of the top quark $\hat{a}_V$ and $\hat{a}_A$ with a sensitivity of the order $\mathcal{O}(10^{-3} - 10^{-2})$. In addition, it is noteworthy that our bounds on the dipole moments of the top quark $\hat{a}_V$ and $\hat{a}_A$ at 1σ are predicted to be of the order $\mathcal{O}(10^{-4} - 10^{-3})$, which is an order of magnitude better than those reported in Refs. [10–21]. Finally, we highlight that the sensitivity with the CLIC data is much stronger than that reported in the literature for the LHC [16] and the ILC [14,15,18] data. In conclusion, despite the fact that the LHC prospects are already strong due to its excellent statistic, the sensitivity of ILC and the CLIC is even stronger.

ACKNOWLEDGMENTS

A. G. R. acknowledges support from SNI and PROFOCIE (Mexico).

[1] W. Bernreuther, R. Bonciani, T. Gehrmann, R. Heinesch, T. Leineweber, P. Mastrolia, and E. Remiddi, Phys. Rev. Lett. **95**, 261802 (2005).
[2] F. Hoogeveen, Nucl. Phys. **B341**, 322 (1990).
[3] M. E. Pospelov and I. B. Khriplovich, Yad. Fiz. **53**, 1030 (1991) [Sov. J. Nucl. Phys. **53**, 638 (1991)].
[4] A. Soni and R. M. Xu, Phys. Rev. Lett. **69**, 33 (1992).
[5] T. Ibrahim and P. Nath, Phys. Rev. D **82**, 055001 (2010).
[6] U. Baur, A. Juste, L. H. Orr, and D. Rainwater, Phys. Rev. D **71**, 054013 (2005).
[7] A. O. Bouzas and F. Larios, Phys. Rev. D **87**, 074015 (2013).
[8] A. O. Bouzas and F. Larios, Phys. Rev. D **88**, 094007 (2013).
[9] Sh. Fayazbakhsh, S. Taheri Monfared, and M. Mohammadi Najafabadi, Phys. Rev. D **92**, 014006 (2015).
[10] D. Atwood, A. Aeppli, and A. Soni, Phys. Rev. Lett. **69**, 2754 (1992).
[11] P. Poulose and S. D. Rindani, Phys. Rev. D **57**, 5444 (1998); **61**, 119902(E) (2000).
[12] S. Y. Choi and K. Hagiwara, Phys. Lett. B **359**, 369 (1995).
[13] P. Poulose and S. D. Rindani, Phys. Rev. D **91**, 093008 (2015).
[14] J. A. Aguilar-Saavedra *et al.*, arXiv:hep-ph/0106315, and references therein.
[15] M. S. Amjad, M. Boronat, T. Frisson, I. G. García, R. Pöschl, E. Ros, F. Richard, J. Rouëné, P. Ruiz Femenia, and M. Vos, arXiv:1307.8102, and references therein.
[16] A. Juste *et al.*, ECONF C0508141 (2005) PLEN0043, and references therein.
[17] D. Asner *et al.*, arXiv:1307.8265, and references therein.
[18] T. Abe *et al.* (American Linear Collider Working Group Collaboration), arXiv:hep-ex/0106057, and references therein.
[19] G. Aarons *et al.* (ILC Collaboration), arXiv:0709.1893.
[20] J. Brau *et al.* (ILC Collaboration), arXiv:0712.1950.
[21] H. Baer *et al.*, arXiv:1306.6352.
[22] B. Grzadkowski, Z. Hioki, K. Ohkuma, and J. Wudka, J. High Energy Phys. 11 (2005) 029.
[23] M. Köksal, A. A. Billur, and A. Gutiérrez-Rodríguez, Adv. High Energy Phys. **2017**, 6738409 (2017).
[24] H. Abramowicz *et al.*, arXiv:1307.5288.
[25] I. F. Ginzburg, arXiv:1508.06581.
[26] I. F. Ginzburg, G. L. Kotkin, S. L. Panfil, V. G. Serbo, and V. I. Telnov, Nucl. Instrum. Methods Phys. Res., Sect. A **219**, 5 (1984).
[27] S. J. Brodsky, T. Kinoshita, and H. Terazawa, Phys. Rev. D **4**, 1532 (1971).
[28] V. M. Budnev, I. F. Ginzburg, G. V. Meledin, and V. G. Serbo, Phys. Rep. **15**, 181 (1975).
[29] H. Terazawa, Rev. Mod. Phys. **45**, 615 (1973).
[30] J. M. Yang, Ann. Phys. (Amsterdam) **316**, 529 (2005).
[31] A. Abulencia *et al.* (CDF Collaboration), Phys. Rev. Lett. **98**, 112001 (2007).
[32] T. Aaltonen *et al.* (CDF Collaboration), Phys. Rev. Lett. **102**, 222002 (2009).
[33] T. Aaltonen *et al.* (CDF Collaboration), Phys. Rev. Lett. **102**, 242001 (2009).
[34] S. Chatrchyan *et al.* (CMS Collaboration), J. High Energy Phys. 01 (2012) 052.
[35] S. Chatrchyan *et al.* (CMS Collaboration), J. High Energy Phys. 11 (2012) 080.
[36] V. M. Abazov *et al.* (D0 Collaboration), Phys. Rev. D **88**, 012005 (2013).
[37] S. Chatrchyan *et al.* (CMS Collaboration), J. High Energy Phys. 07 (2013) 116.
[38] S. C. Inan, Phys. Rev. D **81**, 115002 (2010).
[39] S. C. Inan, Nucl. Phys. **B897**, 289 (2015).
[40] S. C. Inan, Int. J. Mod. Phys. A **26**, 3605 (2011).
[41] I. Sahin and S. C. Inan, J. High Energy Phys. 09 (2009) 069.
[42] S. Atag, S. C. Inan, and I. Sahin, J. High Energy Phys. 09 (2010) 042.
[43] I. Sahin and B. Sahin, Phys. Rev. D **86**, 115001 (2012).
[44] B. Sahin and A. A. Billur, Phys. Rev. D **86**, 074026 (2012).
[45] A. Senol, Int. J. Mod. Phys. A **29**, 1450148 (2014).
[46] A. Senol, Phys. Rev. D **87**, 073003 (2013).
[47] S. Fichet, G. von Gersdorff, B. Lenzi, C. Royon, and M. Saimpert, J. High Energy Phys. 02 (2015) 165.
[48] H. Sun, Phys. Rev. D **90**, 035018 (2014).
[49] H. Sun, Nucl. Phys. **B886**, 691 (2014).
[50] H. Sun, Y. J. Zhou, and H. S. Hou, J. High Energy Phys. 02 (2015) 064.
[51] A. Senol and M. Köksal, J. High Energy Phys. 03 (2015) 139.
[52] S. Atag and A. A. Billur, J. High Energy Phys. 11 (2010) 060.
[53] M. Köksal, V. Ari, and A. Senol, Adv. High Energy Phys. **2016**, 8672391 (2016).
[54] A. Senol and M. Köksal, Phys. Lett. B **742**, 143 (2015).
[55] M. Köksal and S. C. Inan, Adv. High Energy Phys. **2014**, 935840 (2014).
[56] M. Köksal, Eur. Phys. J. Plus **130**, 75 (2015).
[57] A. A. Billur, Europhys. Lett. **101**, 21001 (2013).
[58] M. Köksal, Int. J. Mod. Phys. A **29**, 1450138 (2014).
[59] M. Koksal, Mod. Phys. Lett. A **29**, 1450184 (2014).
[60] V. Ari, A. A. Billur, S. C. Inan, and M. Koksal, Nucl. Phys. **B906**, 211 (2016).
[61] M. Koksal and S. C. Inan, Adv. High Energy Phys. **2014**, 315826 (2014).
[62] I. Sahin and A. A. Billur, Phys. Rev. D **83**, 035011 (2011).
[63] S. C. Inan and A. Billur, Phys. Rev. D **84**, 095002 (2011).
[64] S. Fichet, Acta Phys. Pol. B Proc. Suppl. **8**, 811 (2015).
[65] H. Sun, Y. J. Zhou, and H. S. Hou, J. High Energy Phys. 02 (2015) 064.
[66] J. F. Kamenik, M. Papucci, and A. Weiler, Phys. Rev. D **85**, 071501 (2012).
[67] J. A. Aguilar-Saavedra, Nucl. Phys. **B812**, 181 (2009).
[68] J. A. Aguilar-Saavedra, M. C. N. Fiolhais, and A. Onofre, J. High Energy Phys. 07 (2012) 180.
[69] A. A. Billur and M. Koksal, Phys. Rev. D **89**, 037301 (2014).
[70] A. Gutiérrez-Rodríguez, M. Koksal, and A. A. Billur, Phys. Rev. D **91**, 093008 (2015).
[71] A. Gutiérrez-Rodríguez, M. Koksal, and A. A. Billur*Proceedings, 2015 European Physical Society Conference on High Energy Physics (EPS-HEP 2015): Vienna, Austria, 2015* (SISSA, Trieste, 2015); , *Proc. Sci.*, EPS-HEP2015 (2015) 036.
[72] S. Atag and E. Gurkanlı, J. High Energy Phys. 06 (2016) 118.

[73] ATLAS Collaboration, Report No. ATL-PHYS-PUB-2015-39.
[74] ATLAS Collaboration, Eur. Phys. J. C **71**, 1577 (2011).
[75] CMS Collaboration, Phys. Lett. B **695**, 424 (2011).
[76] CMS Collaboration, Eur. Phys. J. C **71**, 1721 (2011).
[77] K. A. Olive *et al.* (Particle Data Group), Chin. Phys. C **38**, 090001 (2014).
[78] ATLAS Collaboration, Phys. Lett. B **761**, 136 (2016).
[79] V. Khachatryan *et al.* (CMS Collaboration), Phys. Rev. Lett. **116**, 052002 (2016).